

2019

# Quantitative Analysis of Xylene Mixtures Using a Handheld Raman Spectrometer

Lauren Reilly  
Pace University

Follow this and additional works at: [https://digitalcommons.pace.edu/honorscollege\\_theses](https://digitalcommons.pace.edu/honorscollege_theses)

 Part of the [Chemistry Commons](#), and the [Forensic Science and Technology Commons](#)

---

## Recommended Citation

Reilly, Lauren, "Quantitative Analysis of Xylene Mixtures Using a Handheld Raman Spectrometer" (2019). *Honors College Theses*. 263.  
[https://digitalcommons.pace.edu/honorscollege\\_theses/263](https://digitalcommons.pace.edu/honorscollege_theses/263)

This Thesis is brought to you for free and open access by the Pforzheimer Honors College at DigitalCommons@Pace. It has been accepted for inclusion in Honors College Theses by an authorized administrator of DigitalCommons@Pace. For more information, please contact [nmcguire@pace.edu](mailto:nmcguire@pace.edu).

# **Quantitative Analysis of Xylene Mixtures Using a Handheld Raman Spectrometer**

Lauren Reilly

Major: Forensic Science

Advisor: Elmer-Rico Mojica

Department of Chemistry and Physical Sciences

Presentation Date: May 8, 2019

Graduation Date: May 23, 2019



## **Abstract**

Vibrational spectroscopy is the collective term used for both IR (infra-red) and Raman spectroscopy since both techniques measure the vibrational energies of molecules. Although both techniques are non-destructive and non-invasive methods that can provide information about the molecular composition, structure and interactions within a sample, the two can be distinguished based on selection rules. IR take advantage on the change in the dipole moment of the molecular in comparison to Raman which rely on changes in polarizability. In this study, Raman spectroscopy was used to quantitatively determine the composition of xylene mixtures. Different xylene mixtures containing the 3 xylene isomers (m-xylene, o-xylene and p-xylene) were analyzed. The amount of each xylene isomer in mixture was determined by looking at the ratio of areas and intensities of distinct peak found in each isomer over common peak found in all isomers.

## Table of Contents

<b>Content</b>	<b>Page</b>
1. Introduction	4
1.1 Raman Spectroscopy	4
1.2 Raman techniques	5
1.2.1 Dispersive Raman Spectroscopy	6
1.2.2 Fourier Transform Raman Spectroscopy	7
1.2.3 Surface Enhanced Raman Spectroscopy	8
1.2.4 Spatially Offset Raman Spectroscopy	9
1.2.5 Coherent anti-Stokes Raman Scattering	10
1.3 Handheld Raman Spectroscopy	12
1.4 Xylenes	14
2 Materials and Methods	16
2.1 Reagents and Instrumentation	16
2.2 Theoretical Calculations	16
2.3 Procedure	17
3 Results	18
4 Discussion	20
Appendix	27

## **Introduction (1)**

### **Raman Spectroscopy (1.1)**

Raman spectroscopy is an inelastic effect discovered in 1928 by C. V. Raman, which has been used throughout the world as a powerful analytical technique (5). The basic theory behind Raman spectroscopy is that when a sample is irradiated by a laser beam, a portion of photons with a known frequency and polarization are scattered from the sample (1). An inelastic collision occurs between the molecule of the sample and the incident photon from the laser resulting in a change in the vibrational or rotational energy of the molecule (4). This scattered radiation is shifted to a different wavelength and frequency difference between the incident and scattered is what is known as a Raman shift. There are two types of Raman shifts, Stoke lines and anti-Stoke lines. Stokes line occur when the scattered photons are shifted to longer wavelengths due to the molecule gaining energy, while anti-Stoke lines occur when the molecule loses energy and the scattered photons are shifted to shorter wavelengths (5).

The analysis of the frequency shifts of these scattered photons is presented as spectra. The spectra shows lines called spectral bands, which represent the vibrational characteristics for chemical bonds and functional groups that make up the different components in a sample. These spectra provide a type of fingerprint for a specific substance, which favors the analysis of the specific compound due to the fact that no two substances share the same raman spectra (6). This favorability and fingerprinting provides the basis for structural and qualitative analysis. In addition to this, Raman spectroscopy can be used for quantitative determination. It does this by using the linear proportion between the Raman band intensity and the concentration of the corresponding analyte. The equation used by the program to complete the calculation is as follows:  $I_v = I_0 K_v C$ . In

this equation,  $I_v$  is the measured intensity;  $I_0$  is the excitation intensity;  $K_v$  is the constant; and  $C$  is the analyte concentration.

Raman spectroscopy has considerable advantages to other analytical modes including high specificity, shorter timescales, compatibility with aqueous systems, and no need for special sample preparation (5). The lack of sample preparation is one of the reasons that Raman spectroscopy is a nondestructive technique. The other is because it is based on photons of light and energy, which can be measured without altering the sample. One concern may be the interference of the containers used in Raman spectroscopy to hold the samples, however these containers are usually made of glass and plastic neither of which have a strong spectra. In studies concerning quality assurance or in cases such as criminal investigations, this aspect of Raman spectroscopy allows the qualitative and quantitative analysis of samples without exposing them to possible sources of contamination. Water, like plastic and glass also has a very weak Raman spectrum which means that aqueous solutions can be analyzed without the need for separations (6). These characteristics allow analytical chemists across fields to conduct investigatory research in the polymorphs, crystallinity and phase transitions of samples.

### **Raman Techniques (1.2)**

There are a few different techniques used in Raman spectroscopy. Some of these include dispersive Raman spectroscopy, Fourier transform (FT) spectroscopy, surface-enhanced Raman spectroscopy (SERS), spatially offset Raman spectroscopy (SORS) and Coherent anti-Stokes Raman spectroscopy (CARS). The makeup of the Raman spectrometer includes four main parts: a laser source, a sampling system, a detection system, and a computer which collects and saves the data from each run (5).

### **Dispersive Raman Spectroscopy (1.2.1)**

In order to analyze the Raman spectrum, it is necessary to separate the scattered light into each of its component wavelengths (6). To do this in dispersive Raman instruments, the light is focused onto a diffraction grating. This special plate separates the beam of light into its composite wavelengths, which are then directed onto a CCD detector, or charge-coupled device. Another characteristic of dispersive Raman spectroscopy is that it uses visible light or wavelengths of 400nm to 700 nm. There are a few things to consider when choosing a wavelength for a run. Because the Raman intensity has an indirect relationship with wavelength, shorter wavelengths tend to give higher resolution. Fluorescence is also an important factor for choosing wavelength. Increased fluorescence interferes with the sharpness of the Raman data, so a balance must be found when setting the laser level for runs unless the user has a computer software program which corrects for this low level interference. Fluorescence excitation is based on the wavelength of light used (6). This means that if a sample has fluorescent interference at one wavelength it is much less likely to have it at another. Many Raman spectrometers come with multiple laser levels for this reason.

Another key factor for Dispersive Raman spectroscopy is the spectral resolution. The degree of resolution determines the amount of detail the Raman spectrometer can analyze and display in a single spectrum (6). A resolution that is too low provides very little detail and cannot be used for comparisons and identifications. However, when the resolution is adjusted to be too high, the noise interferes with the true spectra of a compound and is also rendered nearly useless. One way to adjust spectral resolution is the use of special gratings within the instrument. Gratings are usually high quality silica that contains multiple grooves which disperse the incident light onto the detector. The width of dispersion is proportionate to the number of grooves on the grating, so more



groves create wider dispersions. In addition to changing the gratings of a spectrometer, changing the optical path length of a spectrograph can increase the resolution of the spectra (6).

### **Fourier Transform (FT) Raman Spectroscopy (1.2.2)**

Both conventional and FT Raman techniques are based on the same basic principle, however FT Raman is unique in two main ways. Instead of visual wavelength FT Raman spectroscopy uses near-IR wavelengths for its laser setting. The second key difference is that FT Raman spectrometers are fitted with Michelson interferometers to analyze the scattered photons (7). An FT Raman spectrometer consists of the following parts: a laser (usually a 1064 nm Nd:YAG ), filters to block Rayleigh scattering, an efficient interferometer, a sensitive detector, and a computer component with the ability to complete fast Fourier-transformations on the acquired interferogram. For FT Raman spectrometer silicon CCD detectors cannot be used and are replaced by single-element, near-infrared detectors (6). Low signal levels cause the spectral noise to mostly consist of detector dark noise, it is considered independent of the Raman intensity. Therefore, the entire spectrum can be sent to the detector which can greatly improve the signal to noise ratio of the spectra and sharpen the results (6).

There are multiple advantages to being built around an interferometer. The Jacquinot and Fellgett are two such advantages and are commonly known as multiplex advantages. These allow the instrument to simultaneously detect multiple wavelengths of light and give it high throughput ability. Being able to analyze multiple wavelengths at one time allows the instrument to obtain a spectrum in a much shorter timeframe and work to offset the decrease in scattering efficiency caused by the longer, near-IR wavelengths (7). In addition to these advantages, FT Raman spectroscopy has increased accuracy in the wavenumbers of the obtained spectra. This allows for

a more accurate calculation if spectra need to be subtracted, which can boost the viability of results (7).

### **Surface Enhanced Raman Spectroscopy (1.2.3)**

Surface Enhanced Raman Spectroscopy or SERS, discovered in 1977, is a technique that offers orders of magnitude increases in Raman intensity, overcoming the traditional drawback of Raman scattering – its inherent weakness. For a long time after its discovery researchers weren't sure how it was able to do this (8). Today it is known that electromagnetic enhancement mechanisms are responsible for most of the SERS processes. This enhancement is caused by light being amplified by localized surface Plasmon resonance (LSPRs) excitation where the concentration of light gathers in the gaps, crevices, or sharp features of plasmonic materials. Substances that can be classified as plasmonic are the noble and coin metals (copper, gold, silver etc.). This enhancement of the Raman spectra can reach factors of  $10^{10}$ - $10^{11}$  in theoretical calculations and usually a enhancement factor of  $10^4$  is enough for researchers to approximate their results (8). However, the enhancement factor seen for a compound is dependent of its structure, so not every run will show the same enhancement. Another factor that was determined to affect the Raman signal is chemical enhancement. Primarily concerned with the transfer of charges, in chemical enhancement the metal-molecule charge transfer state resonates with the excitation wavelength of the spectrometer and enhances the measured signal. These two mechanisms, the electromagnetic and chemical enhancement, contribute to the overall raman enhancement experienced with SERS. The total enhancement is therefore the product of these two mechanisms, which can cause the enhancement factor to reach  $10^{11}$  (8).

There are multiple factors to keep in mind when setting up a SERS run. Raman effects play a large role in experimental runs due to the fact that the dye molecules used possess large

Raman resonance. It is important to choose the correct enhancing substrate for the substance being analyzed as these compounds can be a large variety of shapes and resonances as well as average enhancement factors. During the time period directly following the discovery of SERS there were a lot of issues concerning the substrates to use in experiments. The poorly defined substrates used cause reproducibility problems due to their electrochemical roughening (9). This problem has been continually addressed through the technique of nanofabrication which allows researcher to lessen the electrochemical roughness of the substrates used. Another recent advancement for SERS has been able to let researchers to have greater analyte selectivity by using special surface preparations and modification methods. Due to these advancements and others, SERS is used in a variety of fields as a powerful analytical tool (9).

#### **Spatially Offset Raman Spectroscopy (1.2.4)**

Another Raman technique commonly used by analytical chemists is spatially offset Raman spectroscopy (SORS). This technique diffusely scatters media in order to gain information on the subsurface Raman character of an analyte (10). It is called spatially offset due to the position of collection points along the sample surface that are spatially offset from the illumination point. When this spatial offset is increased, the signal from deeper layers of the analyte is strengthened while the Raman signals from the surface layer are attenuated. Continual adjustment of the spatial offset allows researchers to gain information about nearly all layers of a substance. However, this technique isn't enough to characterize components of a sample lone. The spectra obtained are a mixture of layers from the surface and those deeper in the sample. In order to identify any one layer the mixture needs to be de-convoluted into the components, only then can an identification take place. The method commonly used to separate the mixed spectra is called self-modeling mixture analysis or SMA, which is a special serial algorithm. This algorithm breaks down the

mixed data using an alternating least squares method to obtain the pure spectra of the components as well as their contribution to the overall spectra (10).

### **Coherent anti-Stokes Raman Scattering (1.2.5)**

A relatively new method of Raman spectroscopy is Nonlinear Raman spectroscopic imaging, specifically coherent anti-Stokes Raman Spectroscopy. It works by converting two laser beams into one coherent, high intensity Raman laser by using nonlinear conversions. This Raman beam is centered in the anti-Stokes region and produces scattering emissions of much greater magnitudes than other Raman techniques. The coherent anti-stokes character of the radiation produced through this technique allows analysts to measure the spectra of fluorescent materials as well as gases from discharges, elements of atmospheric chemistry, combustion experiments and plasma (4). This method is one of the more far reaching Raman methods due to its ability to analyze all phases of matter and obtain accurate character and spectral information. During the process, observations of vibrational transition resonances are made through the mixing of two laser beams. CARS is a third order process and can obtain information from isotropic and anisotropic materials, a characteristic not shared by other methods. In addition, the conversion of these lasers into coherently generated photons is much more efficient than in other methods using random scattering. This makes it a good tool for fluorescent substrates.

Because CARS is related to Raman cross sections all measured vibrations seen in the normal Raman spectra will appear in spectra generated by CARS. Despite this, there are multiple factors that differentiate CARS from normal Raman techniques. The first is efficiencies. Because CARS is performed with intense, pulsed sources, as compared to the cw sources used in normal Raman spectroscopy, it produces signals in 0.1 Torr of H<sub>2</sub>. These signals can be 10<sup>11</sup> times higher than normal Raman signals, however this also causes saturation effects that can decrease the

efficiency of CARS. In principle, this should be a straightforward exercise, but in practice the comparison is difficult since normal Raman scattering is usually performed with cw sources, whereas CARS is better carried out with intense, pulsed sources. Other factors that can decrease the efficiency of CARS is the homogeneities of the lasers, and spatial and temporal overlap. If the lasers have inhomogeneities present, or if the spatial and temporal overlaps are not optimized, the efficiency of the CARS output will be detrimentally affected.

Another difference between Coherent anti-Stokes Raman Spectroscopy and normal Raman spectroscopy is in the band shapes, interferences, and dependences obtained in the spectra. The CARS method produces unique band shapes and interferences not seen in normal Raman spectra. These shapes and interferences are caused by background non-resonant susceptibility of the instrument coupled with other neighboring resonances. Another source of these differences comes from CARS property itself, which measures both molecular energies as well as bulk medium similar to the properties of refractive indexes.

One final difference is background interference reduction. This is the most consequential difference for CARS, especially as an analytical tool for characterizing trace amounts of substances. The instrument has to differentiate between background and non resonant signals. The sensitivity of the instrument is dependent of this ability (4). Liquids and solids possess broad line widths, so as long as the concentrations are above one percent of the mixtures components they should be able to be detected. Many CARS instruments have a limit of detection for these substances around one percent, however the ultimate limit of detection will be determined by the solvent and solute and their individual and mixed characteristics. These problems are only associated with low concentrations. Other issues may be involved with low pressure, solvent presence, gas buffers, or low number densities, but those are not included here (4).

This technique allows the analyst to perform molecular imaging without need to create labels. Coherent anti-Stokes Raman scattering (CARS) is a type of nonlinear Raman technique that can perform multiplex analysis by using a broadband laser to create multiple vibrational excitations of the sample. It can also perform analyses using lasers with rapidly alternating wavelengths and may be able to use Fourier Transform methods, although that has yet to be confirmed. One advantage to CARS is that it provides spectral coverage for over 3000 $\text{cm}^{-1}$ , which is considered ultrabroadband (11). This means that the analysis can span the entire region for fundamental vibrational modes without missing or misinterpreting peaks. It does this by combining supercontinuum radiation with the instrument's main, or master, laser that is mode-locked and broadband. Another element capability is the ability for the instrument to send the laser output into a tapered or photonic crystal fiber. This allows the analysis of second and third harmonic generations of the analyte. Research is ongoing to identify additional substances that can be used as tapered fibers (11). Other important factors for instrumentation are the microspectroscopic system, laser repetition rate, and peak intensity optimization. The multiplex capabilities of the CARS system can be greatly improved upon if these features are optimized

### **Handheld Raman Spectroscopy (1.3)**

With the advancements of technologies and scientific methods there had been a demand for more portable analytical devices. Specifically, the handheld Raman spectrometer was in demand for a variety of fields from forensics to art analysis and planetary exploration (20). The ability to carry analytical instruments such as the portable Raman allows investigators and analysts to gain information on a number of substances without the need to move or repackage them. Such substances include street drugs, explosives, and archeological monuments. Handheld instruments

can also be taken to remote areas for instant and accurate analysis of materials that cannot be transported to stationary labs (20).

Criminal activities are one of the main pushes for efficient handheld devices. The drug market has recently seen an influx of designer drugs which can be found in every state. These designer drugs exhibit structural likeness to many illegal substances but also contain other functional groups that make them immune to drug laws. These practices create highly unsafe environments for all involved. One issue with these drugs is that they are not easily classified, however a recent method proposed to solve this is the use of portable Raman devices (21). Handheld surface enhanced Raman spectrometers offer a portable technique for identifications with high sensitivity levels to detect trace amounts of a substance. It has already been validated for drug use, especially methamphetamine and its derivatives (21). There is one complication with the handheld SERS device; it lacks reproducibility of precise results. It is highly important that a method be identified to increase reproducibility without sacrificing sensitivity or low detection limits.

Research including handheld Raman spectroscopy is very important in the present time also due to the increase of terrorism activities and sophisticated explosives. Identifications and characterizations of materials in the field require precise and accurate testing. This is especially true in fields such as forensics, homeland security or future planetary exploration. In forensics the characteristics of a substance determines the possible sentence of the suspect, and is therefore held to a much higher standard than many other sciences. In order to be used in forensic, the handheld devices need to be validated for numerous compounds and elements. It follows the same requirements for explosives testing by the FBI, TSA, or Homeland Security personnel. To

implement the handheld spectrometers it must substantially shown that the method is robust, reproducible, sensitive, and objective, otherwise it cannot be used for drug or explosives testing.

#### **Xylenes (1.4)**

Xylene is a colorless liquid and vapor that is not soluble in water and will float on top of denser water if combined. It is flammable at room temperature and was named after xylong, the Greek word for wood, due to the fact that it was found in crude wood spirit. There are multiple name for xylene including dimethyl benzene, methyl toluene, and xylol (22). The structural build of xylene is two methyl groups attached to a six-carbon ring. There are three main isomers of xylene, called ortho-xylene, meta-xylene and paraxylene

A classic experiment for both vibrational spectroscopic methods deals with xylene isomers. Xylene is a term used for the three isomers of dimethyl benzene. These isomers are the ortho- (o), meta- (m), and para- (p) forms of the molecule (12). These aromatic hydrocarbons are the basis of a variety of organic compounds and are therefore highly important. For example, m-Xylene is used to produce isophthalic acid, which is an important material in dyes, chemical fibers, and other products (12). o-Xylene is to produce phthalic anhydride and synthesize other raw organic materials such as manufacturing paints, and agricultural chemicals (13). p-Xylene is used to production of dimethyl terephthalate synthesize terephthalate, the main raw material used to produce resins, films, and other products.

In 2010, it was estimated that about 44 million tons of xylenes produced, both pure and mixed isomers, and that there was a 10.6% increase in consumption since 2009 (14). The term “mixed xylenes” refers to the equilibrium mixture of four isomers with the same  $C_8H_{10}$  chemical formula with Ethylbenzene being the fourth isomer. One of the chief uses of xylene is as a lubricant, and it is so used in motor oil or brake fluid. Xylene’s powerful solvent properties are



used in printing, rubber and leather processing (22). Xylene is a component of lubricants in motor oil, paints and paint thinners, polishes, waxes, antifreeze, sealants, adhesives, and even gasoline and cigarettes. Xylene is used in some glue. Xylene is also used as a cleaner. These compounds are released into the atmosphere through means such as emissions from industrial sources, exhaust fumes from automobiles, and by volatilization created from their use as solvents. The U.S. National Institute for Occupational Safety and Health has recommended long and short-term exposure limits for xylenes of 100 and 150 ppm, respectively. Short-term inhalation exposure to mixed xylenes in humans results in irritation of the eyes and nose while long-term exposure to mixed xylenes results primarily in central nervous system effects.

## **Materials and Methods (2):**

### **Reagents and Instrumentation (2.1)**

The reagents used in this study consist of the m-xylene isomer (Fisher Scientific, Hampton, NH, USA), o-xylene (Acros Organics, Geel Belgium), and p-xylene (Mallinckrodt, St. Louis, MO, USA) isomers, ethylbenzene (Acros Organics), and commercially available xylenes (Acros Organics). The instruments used were a MiniRam Raman Spectrometer (Model BTR111-785) from B&W Tek, Inc. (Newark, DE, USA) with an excitation wavelength of 785 nm and a spectral range of 175–3150  $\text{cm}^{-1}$ . For the analysis the following settings were used: a laser power level equal to 50 (425 mW), an integration time of 500 s, a time average of 100 s, and multiplier of 5. Each run took approximately 8 min and 20 s and was conducted in triplicate.

The samples were prepared in glass vials where the laser was focused to obtain their Raman spectra. Raman measurements were additionally conducted on a JASCO NRS-3100 confocal dispersive Raman spectrometer equipped with a micro Raman assembly (JASCO, Easton, MD, USA). A 12 mW 488 nm laser was used to induce Raman scattering, which was then collected and detected on a thermoelectrically cooled charge-coupled device detector. A quartz cuvette was used to obtain the Raman spectra of xylene isomers and their mixture at room temperature.

### **Theoretical Calculations (2.2)**

As an aid to the analysis of Raman spectra, theoretical calculations were performed using the Gaussian computer program. Chemical structures were converted to input files using

GaussView 05 (Gaussian Inc., Wallingford, CT, USA) (15). The optimization of geometry and then vibrational frequencies was performed on Gaussian 09 software using the following setting, density functional theory (DFT) approximation implementing the Becke's three-parameter exchange function in combination with the Lee, Yang, and Parr correlation function (B3LYP) (16,17), and the 6-31G basis set. GaussView 05 was then used to analyze the results of these calculations

### Procedure (2.3)

The Raman spectra of xylene mixtures, as well as pure xylene standards for each isomer, ~~as well as pure xylene standards for each isomer~~ were measured. For qualitative analysis, we identified unique peaks for each xylene isomer, which we used as Raman marker bands. Quantitative analysis was performed by normalizing peak intensities of the unique Raman bands relative to a Raman band common to all isomers. This was done by taking the ratio of the intensities ( $I_{norm}$ ) of the distinct band over the common band using the following formula:

$I_{norm} = \frac{\text{peakintensityofuniquepeak}}{\text{peakintensityofcommonpeak}}$ . The normalized intensities of the unique Raman bands of the

xylene mixtures and pure standards were used to quantify each xylene component using the following equation where the Rvalue represents the ratio of xylene component in the mixture:

$R_{value} = \frac{I_{norm,mixture}}{I_{norm,pure}}$ . The composition of commercially available xylenes was also determined

using both a handheld MiniRam Raman spectrometer and the confocal Raman spectrometer.

### Results (3):

Different mixtures of xylene isomers were prepared, and the identity of the isomers present was successfully determined based on the presence of unique peaks associated to each xylene isomer. Figure 2 shows the theoretical Raman spectra from the DFT-based calculations of the individual xylene isomers superimposed with their respective experimental Raman spectra. The theoretical Raman spectra aid in identifying the common and distinct vibrational modes between the xylene isomers.

Raman spectra of the mixtures (three mixtures that are made up of two xylene isomers and one with all three isomers) and individual xylene isomers are shown in Figures 2 and 3. Based on these spectra, common peaks can be seen at  $\sim 1365\text{ cm}^{-1}$  and at the  $\sim 1600\text{ cm}^{-1}$  region that can be assigned as ring vibrational modes. Unique peaks are described as Raman bands that can only be found in one isomer without being overlapped by other Raman bands of another isomer.

A comparison of the standard xylenes' spectra from the confocal Jasco and handheld MiniRam spectrometers is shown in Table 1. This table summarizes the peak assignments of the different observed Raman bands from the handheld MiniRam and confocal Jasco Raman spectrometers. Although there are differences in terms of wavenumber values from both instruments, internal calibration showed a red shift by around  $\sim 15\text{ cm}^{-1}$  in the portable instrument used. The confocal Raman spectrometer was able to detect more Raman bands than the handheld instrument, which was expected considering the difference in sensitivity of the two instruments.

Using the handheld instrument, the mixture containing both m- and o-xylene has peaks at  $527\text{ cm}^{-1}$  corresponding to m-xylene and at  $572$ ,  $1041$ , and  $1210\text{ cm}^{-1}$  corresponding to the o-isomer. The  $527$  and  $1236\text{ cm}^{-1}$  (m-xylene) peaks can also be seen together with peaks at  $632$ ,  $816$ , and  $1192\text{ cm}^{-1}$  (p-xylene) for samples with m- and p-xylene. The unique peaks in each isomer can also be found in a mixture containing the three isomers. There are also peaks that are only common in two out of three isomers such as the one observed at  $\sim 715\text{ cm}^{-1}$  and  $\sim 980\text{ cm}^{-1}$  for both m- and o-xylene (Figure 3). More unique peaks can be seen when the confocal Raman spectrometer is used. In a vibrational window ranging from  $600$  to  $1400\text{ cm}^{-1}$ , the p-xylene has unique peaks at  $649$ ,  $815$ ,  $832$ ,  $1187$ , and  $1208\text{ cm}^{-1}$ , whereas peaks at  $739$ ,  $1057$ , and  $1121\text{ cm}^{-1}$  can be observed only in o-xylene. The m-xylene has unique peaks at the  $730$ ,  $1004$ ,  $1039$ ,  $1253$ , and  $1279\text{ cm}^{-1}$  regions. All of these unique peaks can be observed in binary and tertiary mixtures of xylene isomers (Figure 3). A common peak at around  $1385\text{ cm}^{-1}$  is noticed in all xylene isomers. For the quantitative determination, the tabulated calculations of binary mixtures containing 1:1 volume ratios of two xylene isomers are shown in Table 2.

Background corrected and uncorrected Raman spectra were used on both calculations wherein background corrected means baseline correction of peak intensities while uncorrected Raman spectra means directly using the peak intensities of unique and common peaks. Reproducibility studies using binary mixtures containing equal amounts of xylene isomers showed difference that range from 0 to 10% for most of the unique peaks. For the mixture containing the three isomers, the best unique peak combination is that of  $527$ ,  $572$ , and  $816\text{ cm}^{-1}$  using either the background corrected or uncorrected Raman spectra. A comparison of the calculated ratio of components for each mixture with and without background correction yielded very similar results (Table 2).

## Discussion (4)

Being a hydrocarbon, xylene isomers would have 4 regions where peaks can be observed. The peaks around  $3000\text{ cm}^{-1}$  can be assigned to C-H stretching. Ring modes can be assigned to those peaks found at  $1400\text{--}1600\text{ cm}^{-1}$  region. C-H in-plane bending can be found in the  $1000\text{--}1200\text{ cm}^{-1}$  region. Lastly, out-of-plane C-H bending can be found in the region below  $1000\text{ cm}^{-1}$ .

The Raman spectra of individual xylene isomers revealed several unique peaks for each isomer. For m-xylene, several isolated unique peaks were observed at 527, 1082, 1236, and  $1252\text{ cm}^{-1}$ . For o-xylene, unique peaks were observed at 572, 1041, 1109, and  $1277\text{ cm}^{-1}$ . Lastly, p-xylene has unique peaks at 632, 801, 816, 1171, 1192, and  $1300\text{ cm}^{-1}$  (Figure 2). These peaks were then used as marker bands to qualitatively determine the isomers present in the prepared xylene mixtures. These common and distinct peaks are easy to spot by plotting the spectra in one graph (Figure 3).

The handheld MiniRam spectra have sufficient quality despite its lower sensitivity compared to a more powerful full-sized confocal Raman spectrometer. Despite the lower power and sensitivity of the handheld instrument, it was still able to detect a significant number of Raman bands sufficient for qualitative and quantitative analysis. This is very important, particularly in the application of handheld Raman instruments in quick and simple analytical analyses. From the Raman spectra of the prepared xylene mixtures, several distinct peaks identified in the standard spectra remained isolated and distinct in the spectrum of the mixture.

Initial calculations showed that  $R_{\text{value}}$  utilizing the common peak at  $1365\text{ cm}^{-1}$  yielded a more accurate estimate of the ratio of components as compared to that at  $1600\text{ cm}^{-1}$ . For instance, a mixture of m- and o-xylene showed almost a 1:1 ratio of the two isomers when  $1365$

$\text{cm}^{-1}$  was used as the common peak compared to the 1.8:1 (background corrected) and 1.4:1 (background uncorrected) o-xylene:m-xylene ratio calculated using  $\sim 1600 \text{ cm}^{-1}$ . This is consistently true in other mixtures where a 1:1 calculated ratio was observed when  $1365 \text{ cm}^{-1}$  was used as the common peak, regardless of background correction. The common peak at  $1365 \text{ cm}^{-1}$  was chosen for two reasons. First, this corresponds to peaks observed on both m- and p-xylene with the o-xylene showing a peak at  $1372 \text{ cm}^{-1}$ . The peaks of the three isomers are the same or closer in comparison to the other region ( $1600 \text{ cm}^{-1}$ ) where, m-, o-, and p-xylene are observed at  $1601$ ,  $1594$ , and  $1606 \text{ cm}^{-1}$ , respectively. Another more important reason is the similar peak intensities observed in all xylene isomers in the  $1365 \text{ cm}^{-1}$  region in comparison to the  $1600 \text{ cm}^{-1}$  region where the p-xylene has higher peak intensity. This could be the reason why in mixtures containing p-xylene, the ratio is unusually high. For instance, an almost 1:2 ratio is observed for xylene mixtures containing p-xylene. In terms of unique peaks, any of them can be used with the exception of  $1192 \text{ cm}^{-1}$  observed in p-xylene.

In the absence of fluorescent contaminants, the background is expected to have a minimal contribution to the Raman spectra; therefore, background correction does not seem to be necessary for quicker and simpler data analysis. The only significant difference can be observed in the peak at  $1192 \text{ cm}^{-1}$  found in p-xylene. The values obtained using this peak are significantly different with and without background correction with R values greater than 1 in corrected background. The main reason for this is the presence of another peak at  $1171 \text{ cm}^{-1}$  that overlaps with the peak at  $1192 \text{ cm}^{-1}$  that result in a lower peak intensity in the corrected spectrum.

Table 3 summarizes the quantitative analysis performed on different binary mixtures of xylenes with component ratios other than 1:1. Even at different ratios, the quantitative analysis still yielded R values close to the actual values. Similar to the results in the 1:1 binary mixtures,

the utilization of the  $1365\text{ cm}^{-1}$  Raman band as the common normalizing peak yielded more accurate results. Although any unique peaks can be used for quantitation after several analyses, the best choices of distinct bands for quantitation are the following:  $527\text{ cm}^{-1}$  for m-xylene,  $1041\text{ cm}^{-1}$  for o-xylene, and  $816\text{ cm}^{-1}$  for p-xylene. Reproducibility studies showed variation in signals as high as 20%, which is significantly higher than with the equal volumes of xylene isomers. There is also no significant difference between the results from background corrected and background uncorrected; hence, for data obtained from the confocal Raman spectrometer, background correction was not performed. For the handheld Raman spectrometer, many unique peaks were observed in comparison to the handheld Raman spectrometer. Looking at the spectral window  $600\text{--}1400\text{ cm}^{-1}$ , three unique peaks were used for o-xylene ( $739$ ,  $1057$ , and  $1225\text{ cm}^{-1}$ ) while four peaks were used for m-xylene ( $730$ ,  $1004$ ,  $1253$ , and  $1269\text{ cm}^{-1}$ ) and p-xylene ( $815$ ,  $832$ ,  $1187$ , and  $1208\text{ cm}^{-1}$ ). The common peak found near  $1385\text{ cm}^{-1}$  was used. Since no baseline corrections were performed to look at the ratio of xylene isomers in the confocal Raman spectrometer, the data were processed quickly. Sample calculated Rf values are seen in Table 4 for mixtures containing equal volumes of xylene isomers and in Table 5 for mixtures containing different volumes of xylene isomers

Results show that the values obtained are close to that of actual values, particularly if there is equal volume of xylene isomers. Any unique peaks can be used, especially if multiple analyses are performed, and the reproducibility is better than that of a handheld spectrometer. However, results from mixtures of different volumes of xylene isomers are not as good as those observed in a handheld Raman spectrometer. The main reason for this is the sample analysis in which xylene isomers are mixed and covered within a vial when analyzed by a handheld Raman spectrometer. For the confocal Raman spectrometer, the xylene isomers are mixed beforehand in



a container and then place in a cuvette that is left open during analysis. With these results, the performance of handheld Raman spectrometer is comparable to that of the confocal Raman spectrometer in terms of analyzing mixtures of xylene isomers. The EPA reported that commercial or mixed xylene usually contains about 40–65% m-xylene and up to 20% each of o-xylene, p-xylene, and ethylbenzene (18, 19). Utilizing the same method outlined in the previous section, analysis of a commercial sample of xylene mixture was performed utilizing both the handheld Raman spectrometer and the confocal Raman spectrometer.

The Raman spectra of commercial xylene used in this experiment is shown in Figure 4. The distinct Raman markers for each xylene isomer earlier reported can be observed. With the additional ethylbenzene component, extra distinct peaks not seen in xylene standard spectra can be seen. Some of the additional peaks are bands at 610, 759, 1021, and 1431  $\text{cm}^{-1}$ . These bands are most likely due to ethylbenzene vibrational modes. The Raman spectra of an ethylbenzene standard (also in Figure 4) confirms that these extra peaks are due to ethylbenzene, as they align well with the bands in the ethylbenzene Raman spectra. The quantitative determination of the xylene components utilizing the 1365  $\text{cm}^{-1}$  band as the common peak is summarized in Table 6. The m-xylene was found to be around two times greater than o- and p-xylene components except for the Rf values obtained at 636  $\text{cm}^{-1}$  (background corrected).

The Rf values obtained agree with the data from the EPA. Ethylbenzene does not share the 1365  $\text{cm}^{-1}$  with the xylene isomers, so the quantitative determination of the ethylbenzene component requires a different set of Raman marker bands. For the confocal Raman spectrometer, the R value calculated for m-xylene is, more or less, two times that of o-xylene and p-xylene. This is consistent with the reported amount of xylene isomers found in xylenes. The only exception is that calculated from 1187  $\text{cm}^{-1}$  in p-xylene. The performance of the confocal

Raman spectrometer is similar to that of the handheld Raman spectrometer in terms of obtaining the ratios of different xylene isomers in a commercial xylene.

**Acknowledgements:**

For aiding in experimentation and analysis: Jason Vedad and Ruel Z. B. Desamero, Department of Chemistry, York College and the Institute for Macromolecular Assemblies of the City University of New York, Jamaica, New York 11451, United States and Ph.D. Programs in Chemistry and Biochemistry The Graduate Center of the City University of New York, New York, New York 10016, United States

## Literature Cited

1. Carey, P.R.(1999) Raman Spectroscopy, the Sleeping Giant in Structural Biology, Awakes *The Journal of Biological Chemistry*, 274(38), 26625-26628
2. Kneipp, K.; Kneipp H.; Itzkan, I. (1999) Ultrasensitive Chemical Analysis by Raman Spectroscopy *Chemical Reviews*, 99, 2857-2875
3. Moore, D.S.; Scharff R.J. (2009) Portable Raman Explosives Detection *Los Alamos National Laboratories*.
4. Tolles, W.M; Nibler J.W; McDonald J.R.; Harve, A. (1977) A Review of the Theory and Application of Coherent Anti-Stokes Raman Spectroscopy (CARS), *Applied Spectroscopy*, 31(4), 253-271
5. Yang, D.; Ying, (2011) Applications of Raman Spectroscopy in Agricultural Products and Food Analysis: A Review *Applied Spectroscopy Reviews*, 46, 539–560
6. Hajjou, M.; Qin, Y.; Bradby, S.; Bempong, D.; Lukulay, P. Assessment of the Performance of a Handheld Raman Device for Potential Use
7. Agarwal, U. P.; Atalla, R.H. (1995) FT Raman Spectroscopy: What it is and what it can do for Research on Lignocellulosic Materials, *The 8<sup>th</sup> international Symposium on Wood and Pulping Chemistry*. 3, 67-71
8. Sharma, B.; Frontiera, R.R.; Henry, A.; Ringe, E.; Van Duyne, R.P. (2012) SERS: Materials, applications, and the future, *Materials Today*, 15(1-2)
9. Stiles, P. L.; Dieringer, J. A.; Shah, N. C.; Van Duyne, R. P. (2008) Surface-Enhanced Raman Spectroscopy *Annual Rev. Anal. Chem.* 1:601-626
10. Chao K.; Dhakal, S.; Qin, J.; Peng, Y.; Schmidt, W.F.; Kim, M.S.; Chan, D.E (2017) A Spatially Offset Raman Spectroscopy Method for Non-Destructive Detection of Gelatin-Encapsulated Powders. *Sensors* 17:618-630
11. Yoneyama, H.; Sudo, K.; Leproux, P.; Couderc, V.; Inoko, A.; Kano, H. (2018) CARS molecular fingerprinting using sub-100-ps microchip laser source with fiber amplifier. *APL Photonics* (3)
12. Zhou, Y.; Wu, J.; Lemmon, E. W. Thermodynamic Properties of o-Xylene, m-Xylene, p-Xylene, and Ethylbenzene. *J. Phys. Chem. Ref. Data* 2012, 41, 023103.
13. Bai, Y.; Li, N.; Pei, C.; Yan, Z.; Li, W.; Wei, D. High-Pressure Transformations of Ortho-Xylene Probed by Combined Infrared and Raman Spectroscopies. *Solid State Commun.* 2018, 269, 96–101.
14. Aransiola, E. F.; Daramola, M. O.; Ojumu, T. V. Xylenes: Production Technologies and Uses. In *Xylenes: Synthesis, Characterization and Physicochemical*; Daramola, M. O., Ed.; Nova Publishers: New York, 2013; pp 1–12.
15. GaussView 05; Gaussian, Inc.: Wallingford, CT, 2009.
16. Frisch, M. J.; Trucks, G. W.; Schlegel, H. B.; Scuseria, G. E.; Robb, M. A.; Cheeseman, J. R.; Barone, V.; Mennucci, B.; Petersson, G. A.; Nakatsuji, H.; Caricato, M.; Li, X.; Hratchian, H. P.; Izmaylov, A. F.; Bloino, J.; Zheng, G.; Sonnenberg, J. L.; Hada, M.; Ehara, M.; Toyota, K.; Fukuda, R.; Hasegawa, J.;

- Ishida, M.; Nakajima, T.; Honda, Y.; Kitao, O.; Nakai, H.; Vreven, T.; Montgomery, J. A., Jr; Peralta, J. E.; Ogliaro, F.; Bearpark, M.; Heyd, J. J.; Brothers, E.; Kudin, K. N.; Staroverov, V. N.; Kobayashi, R.; Normand, J.; Raghavachari, K.; Rendell, A.; Burant, J. C.; Iyengar, S. S.; Tomasi, J.; Cossi, M.; Rega, N.; Millam, J. M.; Klene, M.; Knox, J. E.; Cross, J. B.; Bakken, V.; Adamo, C.; Jaramillo, J.; Gomperts, R.; Stratmann, R. E.; Yazyev, O.; Austin, A. J.; Cammi, R.; Pomelli, C.; Ochterski, J. W.; Martin, R. L.; Morokuma, K.; Zakrzewski, V. G.; Voth, G. A.; Salvador, P.; Dannenberg, J. J.; Dapprich, S.; Daniels, A. D.; Farkas, O.; Foresman, J. B.; Ortiz, J. V.; Cioslowski, J.; Fox, D. J. *Gaussian 09*, Revision A.1; Gaussian Inc.; Wallingford, CT, 2009.
17. Lee, C.; Yang, W.; Parr, R. G. Development of the Colle-Salvetti Correlation Energy Formula into a Functional of the Electron Density. *Phys. Rev. B* 1988, 41, 785–789.
  18. Xylenes (Mixed Isomers). <https://www.epa.gov/sites/production/files/2016-09/documents/xylenes.pdf> (accessed January 1, 2018).
  19. Kandyala, R.; Raghavendra, S. P.; Rajasekharan, S. T. Xylene: An Overview of Its Health Hazards and Preventive Measures. *Int. J. Oral Maxillofac. Pathol.* 2010, 14, 1–5.
  20. Viteka, P.; Ali, E.M.A.; Howell, G.M.E.; Jehlicka, J.; Cox, R.; Page, K. (2012) Evaluation of portable Raman spectrometer with 1064 nm excitation for geological and forensic applications *Spectrochimica Acta Part A*, 86:320–327
  21. Mabbott, S.; Correa, E.; Cowcher, D.P.; Allwood, J.W.; Goodacer, R. (2013) Optimization of Parameters for the Quantitative Surface-Enhanced Raman Scattering Detection of Mephedrone Using a Fractional Factorial Design and a Portable Raman Spectrometer. *Analytical Chemistry*. 85:923–931
  22. Dotson, J.D. (2018) Uses of Xylene *Sciencing*

## Appendix

**Table 1. Peaks Assignment of the Observed Raman Bands Obtained from Each Xylene Isomer Using the JASCO Confocal Raman Spectrometer (CRS) and MiniRam Handheld Raman Spectrometer (HRS)**

<i>m</i> -Xylene		<i>o</i> -Xylene		<i>p</i> -Xylene		<i>Assignment</i>
<i>CRS</i>	<i>HRS</i>	<i>CRS</i>	<i>HRS</i>	<i>CRS</i>	<i>HRS</i>	
		510				$\varphi$ ( $\gamma$ CCC)
520	527					$\varphi$ ( $\gamma$ CCC)
541						$\varphi$ breathing
		586	572			$\varphi$ breathing
				649	632	$\varphi$ ( $\gamma$ CCC)
730	713	739	723			$\varphi$ ( $\gamma$ CCC)
				815	801	$\varphi$ breathing
				832	816	$\varphi$ + $\gamma$ C-H
	987	990	973	975		$\gamma$ CH <sub>3</sub>
1004						$\varphi$
1039	1024					$\gamma$ CH <sub>3</sub>
		1057	1041			$\varphi$ breathing
1099	1082					$\varphi$ + $\delta$ C-H
		1121	1109			(ring + CH <sub>3</sub> ) $\gamma$ CH <sub>3</sub>
		1163	1147			$\varphi$ + $\delta$ C-H
1175	1157					$\varphi$ + $\delta$ C-H
				1187	1171	$\varphi$ + $\delta$ C-H
1204				1208	1192	$\varphi$ + $\delta$ C-H
		1226	1210			$\varphi$ + $\delta$ C-H + $\nu$ CH <sub>3</sub>
1253	1236					$\varphi$ + $\nu$ C=C
1269	1252					$\varphi$ + $\nu$ C=C
		1293	1277			$\varphi$ + $\nu$ C=C
				1316	1300	$\delta$ C-H
1381	1365	1387	1372	1381	1365	(CH <sub>3</sub> ) $\delta$ C-H + (ring) $\nu$ C-H
1454	1438	1451	1436	1451	1436	(CH <sub>3</sub> ) $\delta$ C-H
1596	1581	1585	1572	1581	1567	$\varphi$ + $\nu$ C=C + $\delta$ C-H
		1610	1594			$\varphi$ + $\nu$ C=C + $\delta$ C-H
1617	1601			1621	1606	$\varphi$ + $\nu$ C=C + $\delta$ C-H
2730	2720	2730	2720	2731	2722	(CH <sub>3</sub> ) $\nu$ C-H

**Table 1. (Continued). Peaks Assignment of the Observed Raman Bands Obtained from Each Xylene Isomer Using the JASCO Confocal Raman Spectrometer (CRS) and MiniRam Handheld Raman Spectrometer (HRS)**

<i>m-Xylene</i>		<i>o-Xylene</i>		<i>p-Xylene</i>		<i>Assignment</i>
<i>CRS</i>	<i>HRS</i>	<i>CRS</i>	<i>HRS</i>	<i>CRS</i>	<i>HRS</i>	
2862	2862	2856	2850	2862	2862	(CH <sub>3</sub> ) νC-H
		2875	2865			(CH <sub>3</sub> ) νC-H
2916	2907	2917	2907	2919	2909	(CH <sub>3</sub> ) νC-H
	2989	2978	2978			(CH <sub>3</sub> ) νC-H
3009	3110			3011	2997	(ring) νC-H
				3026		(ring) νC-H
3051	3045	3042	3035	3053	3045	(ring) νC-H
		3078				(ring) νC-H
3180	3110	3158	3107		3109	(ring) νC-H
3219	3183	3209	3189	3232	3183	(ring) νC-H

Assignments were based on literature comparisons and DFT-based computer simulations. ν = stretching; φ = ring; δ = in-plane bending; γ = out-of-plane.

**Table 2. Sample Calculated  $R_{value}$  from the Background Corrected and Uncorrected Raman Spectra of the Different Xylene Mixtures Containing Equal Volume Using a Handheld MiniRam Raman Spectrometer**

<i>Xylene Mixture Component</i>	<i>Peak (cm<sup>-1</sup>)</i>	<i>R<sub>value</sub></i>	
		<i>Corrected</i>	<i>Uncorrected</i>
M	527	0.582	0.599
	1236	0.596	0.665
O	572	0.612	0.604
	1041	0.587	0.595
O	572	0.595	0.572
	1041	0.634	0.603
P	632	0.663	0.638
	816	0.688	0.618
	1192	4.021	0.613
M	527	0.473	0.453
	1236	0.461	0.500
P	632	0.548	0.849
	816	0.552	0.478
	1192	3.670	0.480
M	527	0.356	0.407
	1236	0.361	0.466
O	572	0.346	0.385
	1041	0.331	0.383
P	632	0.426	0.475
	816	0.406	0.408
	1192	2.437	0.421

Note: M, *m*-xylene; O, *o*-xylene; P, *p*-xylene.

**Table 3. Sample Calculated  $R_{value}$  from the Background Corrected and Uncorrected Raman Spectra of the Different Xylene mixtures at Different Volume Using a Handheld MiniRam Raman Spectrometer**

<i>Xylene Mixture Component</i>	<i>Peak (cm<sup>-1</sup>)</i>	<i>R<sub>value</sub></i>	
		<i>Corrected</i>	<i>Uncorrected</i>
66.6% M	527	0.607	0.409
	1236	0.800	0.600
33.3% O	569	0.337	0.257
	1041	0.290	0.228
75% M	523	0.809	0.492
	1236	0.843	0.628
25% O	569	0.283	0.225
	1041	0.272	0.206
60% M	523	0.572	0.396
	1236	0.715	0.598
40% O	569	0.429	0.316
	1041	0.390	0.279
66.6% M	527	0.647	0.634
	1236	0.384	0.469
33.3% P	632	0.382	0.388
	816	0.370	0.347
	1192	2.460	0.355
80% M	523	0.630	0.329
	1236	0.813	0.545
20% P	632	0.299	0.232
	816	0.236	0.123
	1192	1.959	0.202
33.3% O	572	0.350	0.358
	1041	0.370	0.346

*Continued on next page.*





**Table 3. (Continued). Sample Calculated  $R_{value}$  from the Background Corrected and Uncorrected Raman Spectra of the Different Xylene mixtures at Different Volume Using a Handheld MiniRam Raman Spectrometer**

<i>Xylene Mixture Component</i>	<i>Peak (cm<sup>-1</sup>)</i>	<i>R<sub>value</sub></i>	
		<i>Corrected</i>	<i>Uncorrected</i>
66.6% P	632	0.782	0.777
	816	0.843	0.664
	1192	5.127	0.671
20% O	572	0.341	0.079
	1041	0.367	0.221
80% P	632	0.789	0.236
	816	0.818	0.079
	1192	5.096	0.291
66.6% O	572	0.779	0.790
	1041	0.773	0.789
33.3% P	632	0.416	0.436
	816	0.409	0.412
	1192	2.262	0.426

Note: M, *m*-xylene; O, *o*-xylene; P, *p*-xylene.

**Table 4. Sample Calculated  $R_{value}$  from the Background Corrected and Uncorrected Raman Spectra of the Different Xylene Mixtures Containing Equal Volume Using a Confocal Raman Spectrometer**

<i>Xylene Mixture Component</i>	<i>Peak (cm<sup>-1</sup>)</i>	<i>R<sub>value</sub></i>
50% M	730	0.741
	1004	0.742
	1253	0.707
	1269	0.774
50% O	739	0.894
	1057	0.814
	1226	0.783
50% M	730	0.618
	1004	0.622
	1253	0.587
	1269	0.596
50% P	815	0.503
	832	0.479
	1187	0.510
	1208	0.470
50% O	739	0.653
	1057	0.640
	1226	0.639
50% P	815	0.791
	832	0.756
	1187	0.806
	1208	0.759
33% M	730	0.462
	1004	0.460
	1253	0.448
	1269	0.507

*Continued on next page.*

**Table 4. (Continued). Sample Calculated  $R_{value}$  from the Background Corrected and Uncorrected Raman Spectra of the Different Xylene Mixtures Containing Equal Volume Using a Confocal Raman Spectrometer**

<i>Xylene Mixture Component</i>	<i>Peak (cm<sup>-1</sup>)</i>	<i>R<sub>value</sub></i>
33% O	739	0.566
	1057	0.529
	1226	0.517
33% P	815	0.468
	832	0.424
	1187	0.506
	1208	0.426

Note: M, *m*-xylene; O, *o*-xylene; P, *p*-xylene.

**Table 5. Sample Calculated  $R_{value}$  from the Uncorrected Raman Spectra of the Different Xylene Mixtures at Different Volumes Using a Confocal Raman Spectrometer**

<i>Xylene Mixture Component</i>	<i>Peak (cm<sup>-1</sup>)</i>	<i>R<sub>value</sub></i>
67% M	730	0.887
	1004	0.903
	1253	0.857
	1269	0.885
33% O	739	0.521
	1057	0.459
	1226	0.448
67% M	730	0.683
	1004	0.701
	1253	0.678
	1269	0.683
33% P	815	0.402
	832	0.368
	1187	0.399
	1208	0.365

*Continued on next page.*

**Table 5. (Continued). Sample Calculated  $R_{value}$  from the Uncorrected Raman Spectra of the Different Xylene Mixtures at Different Volumes Using a Confocal Raman Spectrometer**

<i>Xylene Mixture Component</i>	<i>Peak (cm<sup>-1</sup>)</i>	<i>R<sub>value</sub></i>
67% O	739	0.954
	1057	0.933
	1226	0.909
33% P	815	0.458
	832	0.408
	1187	0.513
	1208	0.419
33% O	739	0.398
	1057	0.391
	1226	0.387
67% P	815	0.893
	832	0.881
	1187	0.902
	1208	0.873
20% O	739	0.326
	1057	0.321
	1226	0.369
80% P	815	0.347
	832	0.340
	1187	0.653
	1208	0.113
60% M	730	0.775
	1004	0.792
	1253	0.755
	1269	0.814

*Continued on next page.*

**Table 5. (Continued). Sample Calculated  $R_{value}$  from the Uncorrected Raman Spectra of the Different Xylene Mixtures at Different Volumes Using a Confocal Raman Spectrometer**

<i>Xylene Mixture Component</i>	<i>Peak (cm<sup>-1</sup>)</i>	<i>R<sub>value</sub></i>
40% O	739	0.767
	1057	0.699
	1226	0.677
75% M	730	0.933
	1004	0.948
	1253	0.905
	1269	0.925
25% O	739	0.382
	1057	0.331
	1226	0.325
80% M	730	0.786
	1004	0.805
	1253	0.778
	1269	0.766
20% P	815	0.303
	832	0.271
	1208	0.270

Note: M, *m*-xylene; O, *o*-xylene; P, *p*-xylene.

**Table 6. Calculated  $R_{value}$  from the Raman Spectra of Commercial Xylene Obtained Using a Handheld MiniRam Raman Spectrometer and Confocal Raman Spectrometer**

<i>Xylene Mixture Component</i>	<i>Peak (cm<sup>-1</sup>)</i>	<i>R<sub>value</sub></i>		<i>Comments</i>
		<i>Corrected</i>	<i>Uncorrected</i>	
M	523	0.466	0.410	Except for the 636 cm <sup>-1</sup> in corrected spectra, all other distinct peaks gave acceptable $R_{values}$
	1236	0.515	0.546	
O	569	0.243	0.205	
	1041	0.261	0.238	
P	636	0.091	0.251	
	816	0.258	0.237	
<i>Confocal Raman Spectrometer</i>				
M	730	0.618		All distinct peaks gave acceptable $R$ values except the one at 1187 for <i>p</i> -xylene.
	1004	0.733		
	1253	0.614		
	1269	0.704		
O	739	0.382		
	1057	0.362		
	1226	0.355		
P	815	0.384		
	832	0.310		
	1187	0.504		
	1208	0.356		

Note: The 1365/1385 cm<sup>-1</sup> Raman band was used as the common normalizing peak. M, *m*-xylene; O, *o*-xylene; P, *p*-xylene.

## **Figure Table:**

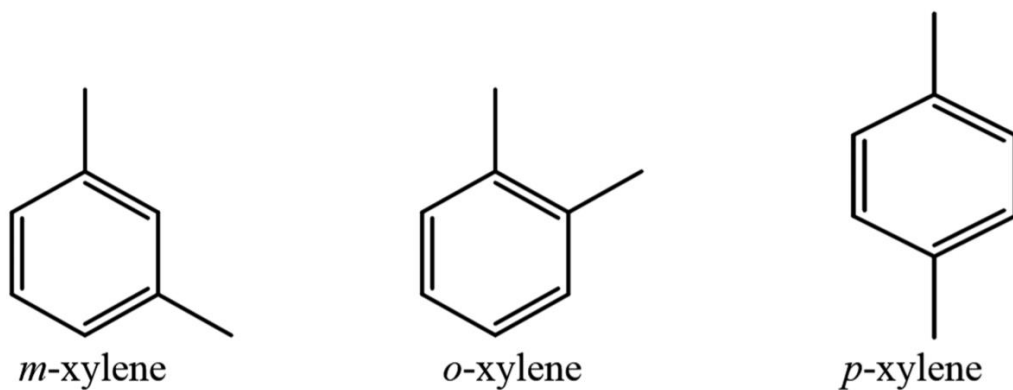
Figure 1: Xylene isomers used in the study.

Figure 2: Raman spectra of xylene isomers obtained from the confocal Jasco Raman instrument superimposed with DFT-based calculated Raman spectra (2500x)

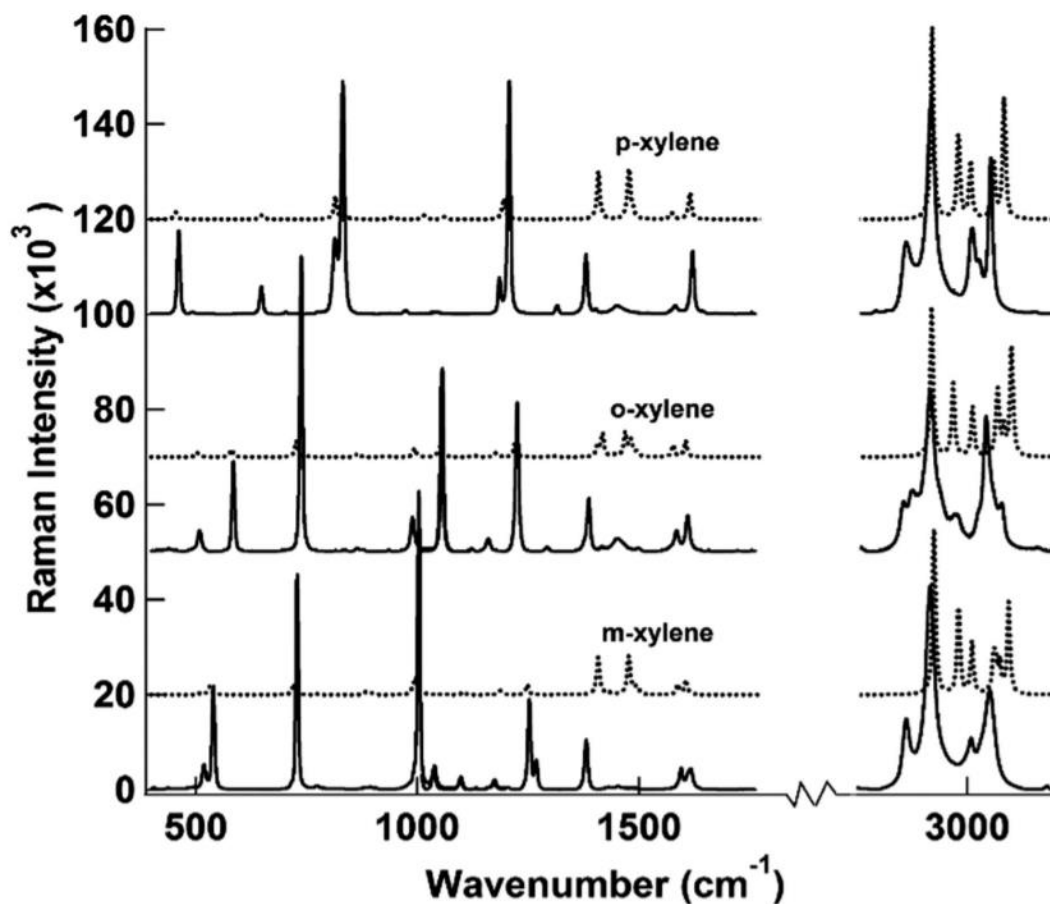
Figure 3: Raman spectra of the individual xylene isomers and different xylene mixtures at 1:1 v:v ratios taken using the handheld MiniRam instrument and confocal Raman spectrometer

Figure 4: Raman spectra of a commercial xylene mixture and ethylbenzene measured using a handheld MiniRam Raman instrument and the confocal Raman spectrometer





**Figure 1:** Xylene isomers used in the Study



**Figure 2:** Raman spectra of xylene isomers obtained from the confocal Jasco Raman instrument (solid line) superimposed with DFT-based calculated Raman spectra (2500x) (broken line)

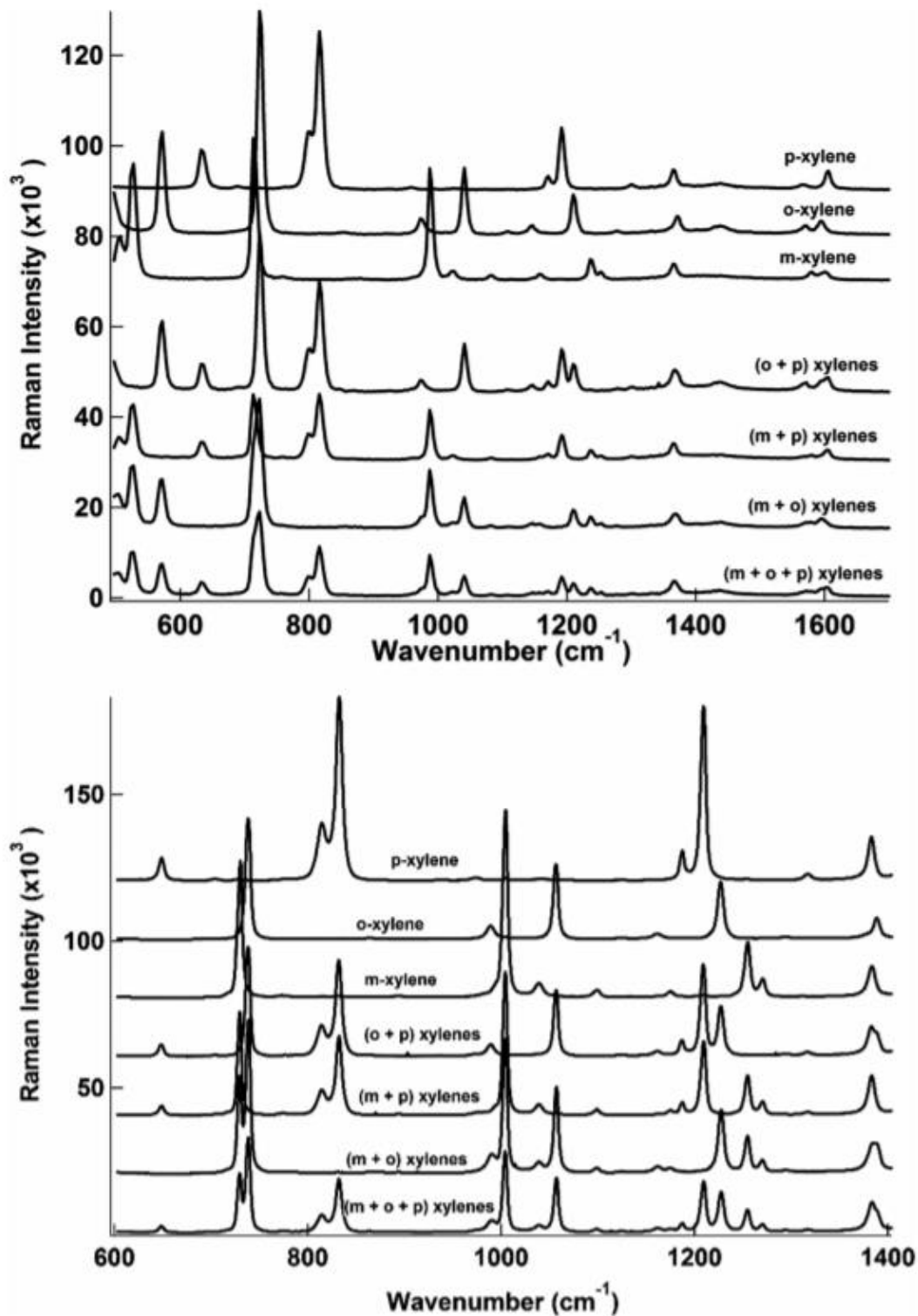


**Figure 3:** Raman spectra of the individual xylene isomers and different xylene mixtures at 1:1 v:v ratios taken using the handheld MiniRam instrument (top) and confocal Raman spectrometer (bottom).

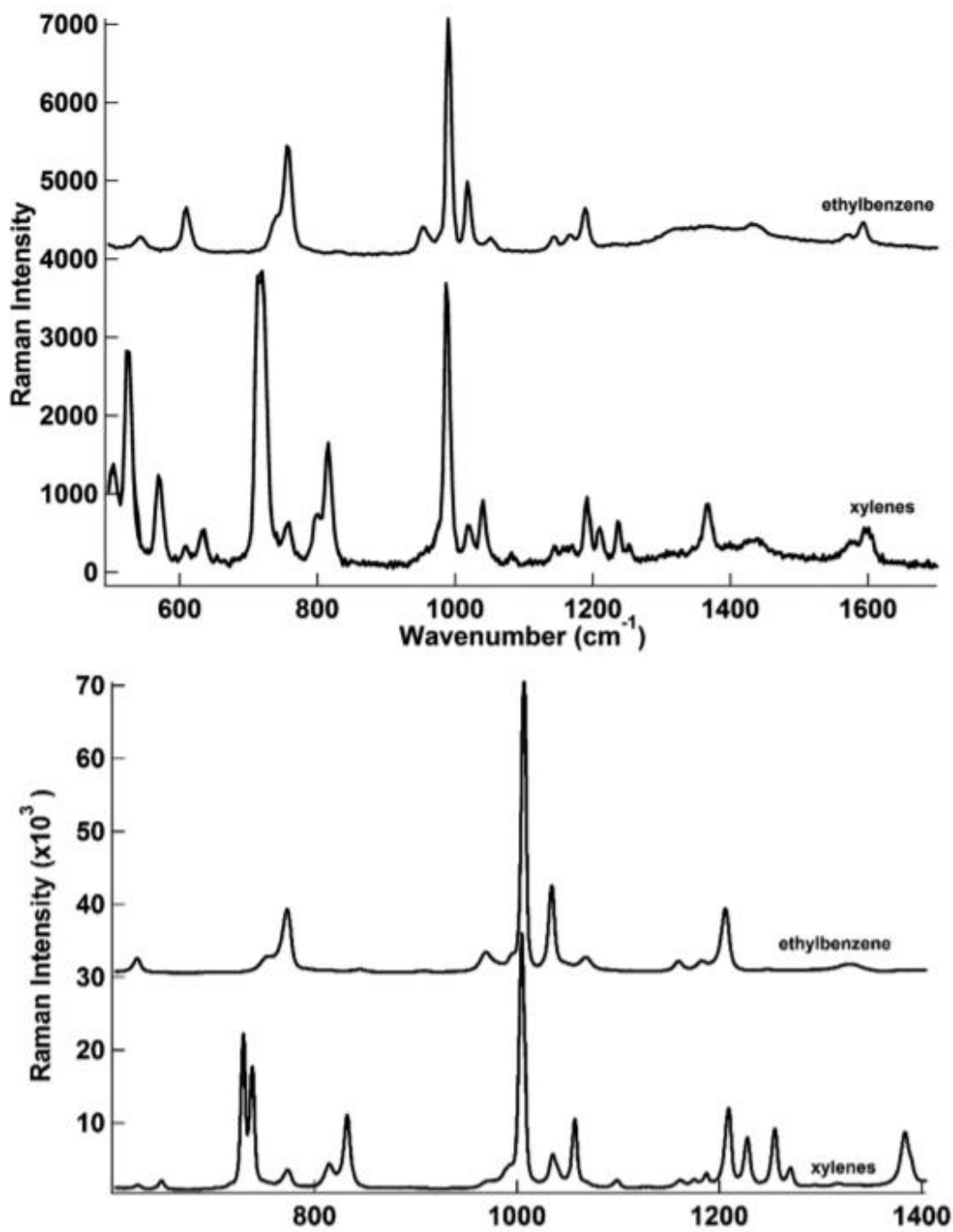


**Figure 4:** Raman spectra of a commercial xylene mixture and ethylbenzene measured using a handheld MiniRam Raman instrument (Top) and the confocal Raman spectrometer (Bottom)